Evaluation of enzyme immobilization strategies on biosensor performance

Yashda Singh[1], Shikha Sharma[1,3] and Sudha Srivastava[1,2*]

[1]Department of Biotechnology, Jaypee Institute of Information Technology, A-10, Sector-62, Noida-201309, INDIA

[2]Department of Chemistry, Jaypee Institute of Information Technology, A-10, Sector-62, Noida-201309, INDIA

[3]Current Address: IQVIA – VC Lab, Toronto, Ontario, Canada. *Corresponding author: sudha.srivastava@mail.jiit.ac.in

Abstract

Biosensor efficiency is highly dependent on the effective integration of biological entities with materials and sensing technology, besides the enzyme loading capacity of the material. Variability in critical parameters governing biosensor efficiency poses difficulty in the fair evaluation of reported literature related to diverse methods and materials for enzyme immobilization. Recent advances in nanotechnology have led to a comparison of traditional materials with nanomaterials for the immobilization of biocatalysts. The present study shows that enzyme immobilization is optimum in covalently bound enzyme, while the 3-D conformation of the enzyme is preserved through optimum curvature of nanoparticles. Further, the shape and approachability of nanostructures to the enzyme active center facilitate faster electron transfer for efficient electrochemical biosensing. The Gox-AuNPs modeified gold electrode showed 1.7 times higher current response and greater senstivity 22.42 μA mM^{-1} cm^2 than Gox-Fe_3O_4NPs with senstivity 14.3 μA mM^{-1} cm^{-2} . After 60 days of storage at 25 ºC the Gox-AuNPs retained 73% of its initial response whereas Gox- Fe_3O_4NPs retained 56%, indicating improved storage and enzymatic stability.

Keywords: Nanomaterials; Enzyme Immobilization; Biosensor; Membrane

1. Introduction

Biosensor research has progressed significantly since the development of the first enzymebased sensing system in 1962, by Clark and Lyons. They sandwiched a thin layer of glucose oxidase (GOx) enzyme between a semipermeable dialysis membrane [1]. Since then, the fabrication of an enzymatic biosensor has been the topic of significant research. The choice of support matrix and the immobilization method depend on the intended application, thereby influencing the sensitivity, specificity, and response time, overall affecting the efficiency of the enzymatic biosensor [2].

Enzymes are sensitive to changes in pH, temperature, and other environmental conditions. Different methods of enzyme immobilization on solid support matrices include adsorption, cross-linking or covalent bonding, matrix entrapment, and membrane encapsulation [3]. The selection of materials and methods can affect functional characteristics, such as enzyme stability, catalytic activity, minimum leaching, binding, and loading capacity. Incorporation of certain selective membranes like cellulose acetate, polyvinylpyrrolidone (PVP) polymer [4], nafion membrane [5], and Poly-m-phenylenediamine (PPD) [6] was used to reduce the interference from other species, but an increase in response time was recorded due to the delayed diffusion rate [7]. In recent years, alternative support matrices, including polymeric

material and nanoparticle-integrated substrates, have been investigated to improve the efficiency of enzymatic biosensors. Varieties of support matrices are used for enzyme immobilization, which essentially depends on the type and catalytic property of the enzyme. Broadly, support material can be classified into organic type (Biopolymers, synthetic polymers, organic nanoparticles) and inorganic type (inorganic polymers, metal nanoparticles like gold, copper, zinc, and magnetic nanoparticles) [8]. Replacing membranes with nanomaterials such as gold, nickel, magnetic nanoparticles, silica nanoparticles, etc., has revolutionized biosensor research by dropping the response time to seconds and increasing the sensitivity range [9].

Ge et al. immobilized gold nanoparticles (GNP-Gox) on a modified interdigitated electrode (IDE) for the detection of glucose using glucose oxidase enzyme, which was compared with graphene (graphene-Glucose oxidase enzyme). A two-fold increase in the limit of detection (LOD) was observed from 0.06 to 0.03 mg/mL for GNP-Gox [10]. Recent study published by *Gigli et. al.* developed interference-free biosensor for the detection of catecholamine using tyrosinase enzyme immobilized using chitosan with the sensitivity of 0.583 $\mu A\ \mu M^{-1}\ cm^{-2}$ and 0.17 μM limit of detection with fast response time [11]. Electrospun nanofiber (diameter of 280 nm)of polypyrrole-chitosan due to porous and large surface area was used for the detection acetylcholine offering LOD of 5 μM and a reliable performance of over 30 days [12]. Poly(Nphenylglycine), a biocompatible polymer was used to construct a flexible wearable continuous glucose monitoring (CGM) system including diffusion-limiting membrane polyurethane.

PPG/Gox film was crossliked with glutaraldehyde, offering sensitivity of 12.69 $\mu A\ mM^{-1}\cdot cm^{-2}$ and an excellent linear range of 1-30 mM with 30 days stability [13]. Direct conjugation of the enzyme onto the magnetic nanoparticles, owing to their unique characteristics such as superparamagnetic, high surface-to-volume ratio, low toxicity, and ease in the separation process, justifies their frequent use in an enzymatic biosensor. The governing factors for the versatility of the nanoparticle are the shape, size, pH, temperature, and strength of the nanomaterials, in addition to other physical and chemical properties [14].

Here, we present a comparative analysis of enzyme immobilization using different support matrices and nanoparticles with a suitable immobilization technique. As a model system for the comparative analysis of enzymatic biosensor fabrication, we have used glucose oxidase (GOx) enzyme.

Table 1: Development of enzymatic biosensors with various membranes and nanostructures

Type of support for Immobilization	Sensitivity ($\mu A\ mM^{-1}\ cm^{-2}$)	Detection limit (μM)	Linear range (mM)	Response time (sec)	Storage Stability	Refer ence
Polypyrrole	Data not reported	Data not reported	1-10	20-40	30% decrease in 20 days	[15]
Cellulose acetate	Data not reported	Data not reported	27	100	6 days	[16]
Polysiloxanes	0.012	0.06	0–18	60	51 days	[17]

Eggshell membrane	NA	0.1	0.5 - 10	120	2 months	[18]
Polypyrrole crosslinked chitosan	0.58	0.068	1 - 20	4	50 days	[19]
Chitosan-entrapped mesoporous carbon nanocomposite	56.12	4.1	0.25- 3	Data not reported	Data not reported	[20]
Chitosan	9.17	77.0	0.1–5	2	8 days	[21]
TiO_2 nanoparticlemodified CNT	5.46	Data not reported	0.3- 1.5	Data not reported	30 days	[22]
Gold nanoparticle	6.1	15	0.02–14	7	4 days	[23]
glycerol-3-phosphate oxidase and glycerol kinase on GO-NP modified pencil graphite(PG) electrode.	121.45	0.002	0.001 - 60	Data not reported	210 days	[24]
Porous poly (acrylonitrile-coacrylic acid)	6.82	0.5	0.005- 3	30	5 weeks	[25]
Gold nanorods with cellulose acetate composite film	8.4	20	0.03 -2.2	Data not reported	20% decrease in 30 days.	[26]
Magnetic Ni nanoparticles (GOx-NiNP/N)	6.92	7.3	Data not reported	Data not reported	15 days (72 %)	[27]
Nafion membrane with multi-walled carbon nanotubes	167	17	0.01–3.5	Data not reported	120 days	[28]
Polyacrylic acid (PAA) with GoxCNT film	34	10	0.01–5	Data not reported	14 days	[29]

MXene polynanogel	48.9 8	3.1	0.03–16.5	Data not reported	Data not reported	[30]

2. Materials and methods

2.1 Nanoparticles Synthesis

Nanoparticles of gold and magnetite were synthesized using the chemical methods given below.

2.1.1 Magnetite Nanoparticles Synthesis

Zhu's co-precipitation method was used for the synthesis of magnetite nanoparticles with ferrous and ferric salts under an alkaline environment [31]. The reaction mechanism of magnetite nanoparticle synthesis is discussed below.

$$Fe^{3+} + H_2O \xrightarrow{deprotonation} Fe(OH)_x^{3-x} \quad (6)$$

$$Fe^{2+} + H_2O \xrightarrow{deprotonation} Fe(OH)_y^{2-y} \quad (7)$$

$$Fe(OH)_x^{3-x} + Fe(OH)_y^{2-y} \xrightarrow{oxidation\ /dehydration} Fe_3O_4 \quad (8)$$

2.1.2 Gold nanoparticles Synthesis

Synthesis of gold nanoparticles was done as reported in our previous work [32]. The underlying reaction mechanism of gold nanoparticle synthesis is discussed below.

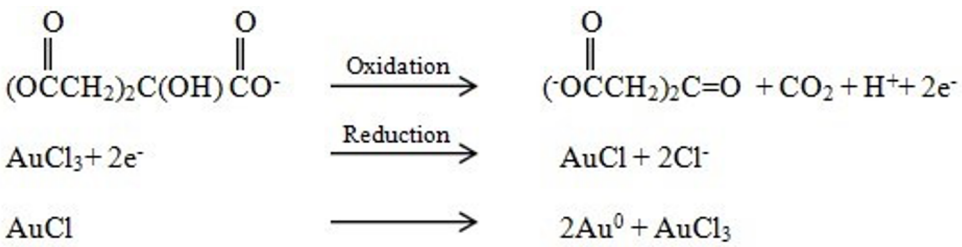

2.2 Enzyme Immobilization

Glucose oxidase (GOx) was immobilized on different platforms using covalent, electrostatic, entrapment and crosslinking methods.

2.2.1 Immobilization of glucose oxidase on AuNPs by electrostatic interaction

Scheme 1 shows the methodology of gold nanoparticles synthesis and modifications thereof to ensure electrostatic binding of enzyme. The gold nanoparticles stabilized with citrate (AuNPs) were dispersed in a solution of poly diallyl dimethyl ammonium chloride (PDADMAC). To achieve the uniform functionalization, 3mL fresh solution of the AuNPs (10 pmol/ml) was stirred with 1 mL PDADMAC in 3mL water for 2 h. The polyelectrolyte modified AuNPs were then centrifuged and 20U of Glucose oxidase (GOx) was added to the pellet. Mixture was centrifuged at 12000 rpm at 4ºC for 20 minutes to separate free enzyme (GOx) from the immobilized (GOx-AuNPs).

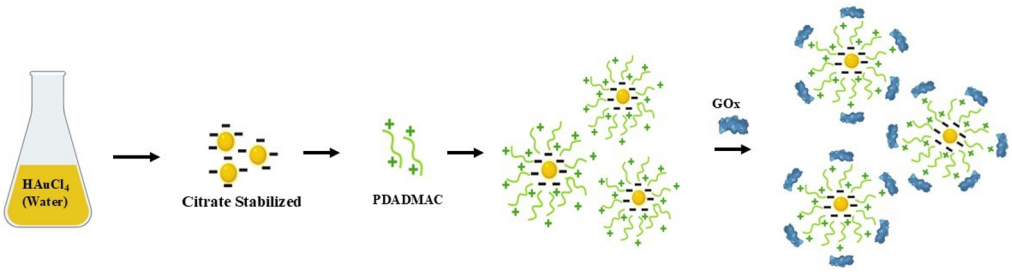

Scheme 1: Schematic illustration of gold nanoparticles synthesis and functionalization for electrostatic immobilization of enzyme.

2.2.2 Immobilization of Glucose oxidase on nanoparticles by covalent interaction (Fe_3O_4 and Au NPs)

Immobilization of enzyme onto magnetite and gold nanoparticles is shown in Scheme 2(a-b) . The Fe_3O_4NPs were coated with 3-aminopropyltriethoxysilane (3-APTES), while that of AuNPs underwent modification with 3-aminopropanethiol (3-APT) [33]. Subsequently, 4ml of glutaraldehyde solution (10% glutaraldehyde) was added to the NPs suspension and stirred continuously for 1 h. To the pellet, 20U of Glucose oxidase (GOx) was added, and the mixture was incubated overnight with constant stirring at 4 °C. The GOx-NPs complex thus obtained was resuspended and stored in 1 ml phosphate buffer solution (PBS), pH 6.5, at 4 °C.

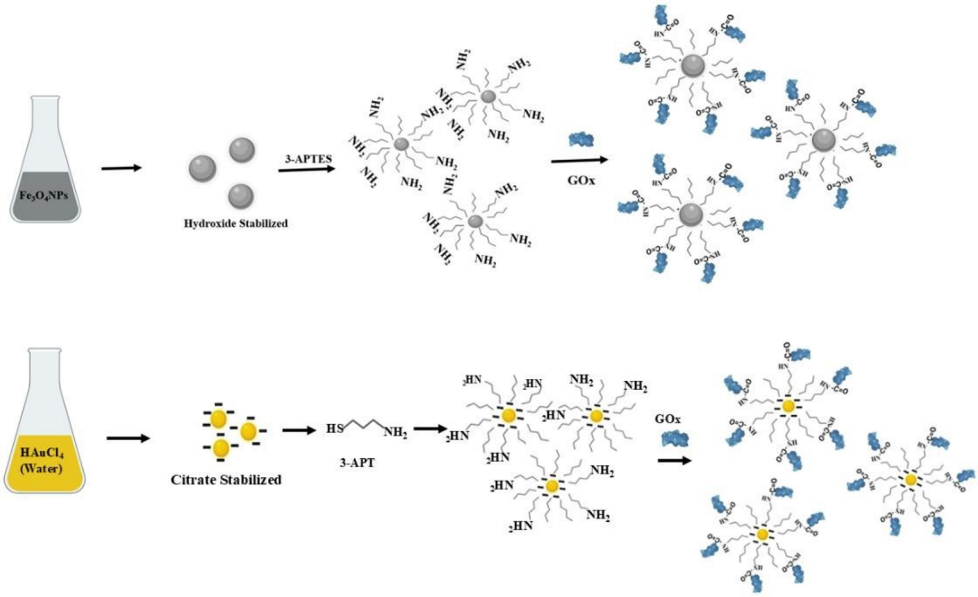

Scheme 2: Schematic representation of covalent immobilization strategy of enzyme onto a) Magnetite nanoparticles and b) Gold nanoparticles

2.2.3 Physical adsorption of GOx on PVDF and NC membranes

10 µl of GOx solution (20U/10 µl) was immobilized onto a 2 cm^2 piece of Polyvinylidene Fluoride (PVDF) and nitrocellulose (NC) membranes (0.45 µm), slowly allowing each drop to dry before adding the next drop. The membrane was air-dried at room temperature for 1-2 hours and stored at 4 °C for further use(as shown in Scheme 3).

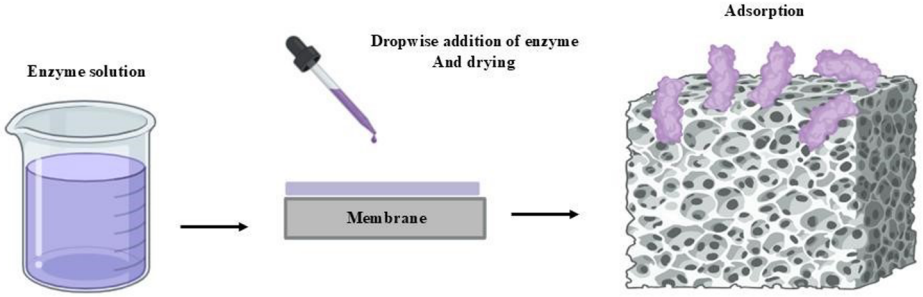

Scheme 3: Schematic representation of physical adsorption of enzyme onto PVDF or NC membrane.

2.2.4 Entrapment of GOx in calcium alginate beads

Buffer solution containing 20 units of GOx was mixed well with 3% Na-alginate solution. This was followed by dropwise addition of the same in a 0.2M $CaCl_2$ solution with the help of a syringe kept just above the surface of the calcium chloride solution to ensure sphericity of the beads. The spherical beads of enzyme entrapped in calcium alginate gel were left undisturbed

for 2 hours for hardening (see Scheme 4). Afterwards, the excess calcium chloride solution was decanted off and replaced by autoclaved milliQ water and stored at 4 °C till further use.

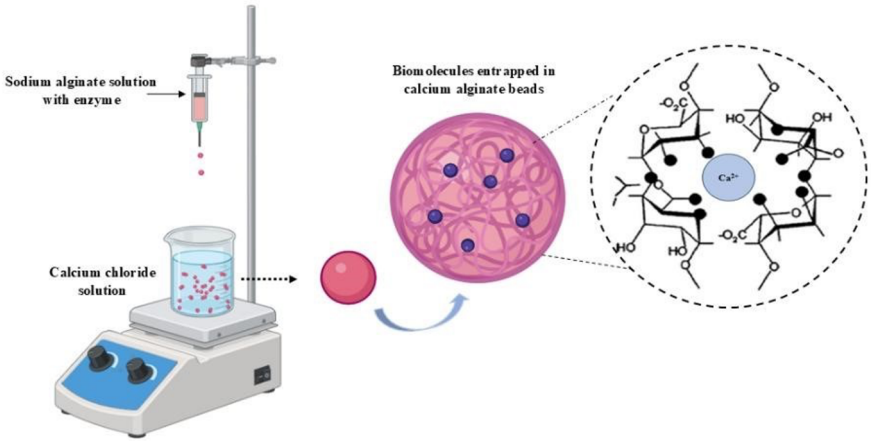

Scheme 4: Entrapment of enzyme through calcium alginate beads formation.

2.2.5 Entrapment of GOx in polyacrylamide gel

For the entrapment of 20 U of GOx, 15 % of polyacrylamide gel was prepared by 7.5 g of acrylamide, 0.5 g of bisacrylamide, 50 mg of APS along with 20 U of enzyme was added to 25 ml of 0.1 M of phosphate buffer (pH 6.8) with 50 ul of TEMED gently poured into $_{petri}$ dish and left to polymerize at room temperature for 1 hour. After this the gel was crushed into pieces and resuspended in phosphate buffer [34].

2.3 Estimation of GOx immobilization efficiency, activity and leaching

After GOx immobilization on different matrices, phosphate buffer (pH 6.5) was used to wash the support matrices. The washout buffer solution was collected in a tube, and the amount of free enzyme was estimated. In the case of entrapment methods, i.e., the calcium alginate beads were cut open and resuspended in phosphate buffer, while in the case of polyacrylamide gel, the pieces were crushed and resuspended in phosphate buffer, followed by enzyme activity analysis. Here, the amount of enzyme per bead (or gel piece) was calculated based on the total number of beads or gel pieces formed. The percentage immobilization of the enzyme was calculated

$$\%\mathbf{Immobilization} = \frac{\text{Total GOx activity} - \text{GOx activity in supernatant}}{\text{Total GOx activity}} \times 100$$

2.3.1 Activity analysis of free and immobilized enzyme

Enzyme activity was assayed using dinitrosalicylic acid (DNS) colorimetric method [35] for temperatures ranging from 25°C - 65°C. The expected reaction and byproducts are mentioned below;

$$\beta\text{–D–Glucose} + \text{Glucose oxidase–FAD} \rightarrow \beta\text{–D–Gluconolactone} + \text{Glucose oxidase–FADH}_2$$

$$\text{Glucose oxidase}-FADH_2+O_2 \rightarrow \text{Glucose oxidase}-FAD+H_2O_2$$

$$\beta-D-\text{Glucose} + 3,5-\text{dinitrosalicylic acid} \rightarrow 3-\text{amino}, 5-\text{nitrosalicylic acid} + \text{Gluconic acid}$$

2.3.2 Enzyme Leakage

The stability of immobilized enzyme in terms of percentage loss or leakage of

$$\text{Percentage leakage of GOx} = \frac{\text{GOx activity}_{0\ h} - \text{GOx activity}_{72\ h}}{\text{GOx activity}_{0\ h}}$$

enzyme was assessed by comparing the immobilized enzyme activity at 0 hours and after 72 hours. During the 72-hour storage time, the immobilized enzyme was washed thrice daily with phosphate buffer, pH 6.5.

2.4 Biosensor Fabrication

The biosensors were fabricated following the procedure described in our previous work [36]. Briefly, the working area of the gold screen-printed electrode (SPE) was activated using 10 µl of 3 APT (10mM). On to this, further modification was done using 10 µl of glutaraldehyde (2.5%), following by the addition of amino functionalized NPs (10pmol/ml) and allowed it to dry for 2 hrs [37]. Finally, 20U of Glucose oxidase was layered on the nanoparticles modified electrode surface. The fabricated biosensor was rinsed with water, dried and stored in PBS (pH 6.5) at 4°C for further use. Cyclic voltammetry (CV) and impedance (EIS) were subsequently used after each surface modification. The morphology of synthesized NPs was examined using a transmission electron microscope (JEOL 2100F). Ultraviolet and visible (UV-Vis) absorption spectra of NPs dispersion were recorded on an ND 1000 UV–Vis Spectrophotometer (Nanodrop technologies) operated at 12 V.

3. Results and Discussion

Parameters known to influence the activity of immobilized enzymes were examined, specifically, the matrix and method of immobilization. Traditional support materials for immobilization of enzymes, like membranes/thin film (PVDF and NC) and polymeric encapsulation (Na-alginate beads and polyacrylamide gel), were compared with nanoparticles (gold and magnetite). The synthesized nanoparticles (Au and Fe_3O_4NPs) were characterized physically and chemically, followed by activity analysis of covalently and electrostatically immobilized enzyme (GOx) onto these nanoparticles.

3.1 Characterization of Nanoparticles for Immobilization

The characterization of gold nanoparticles (AuNPs) and magnetite nanoparticles (Fe_3O_4NPs) was done using UV-Visible spectroscopy and transmission electron microscopy (TEM), as shown in Figure 1. Gold nanoparticles show a characteristic absorption peak at 523 nm (Figure 1A) while magnetite nanoparticles (Figure 1B) show an absorption maximum at 400 nm. The

shift in the absorption peak wavelength, in comparison to bulk particles, gives a qualitative idea of the size of the synthesized particles.

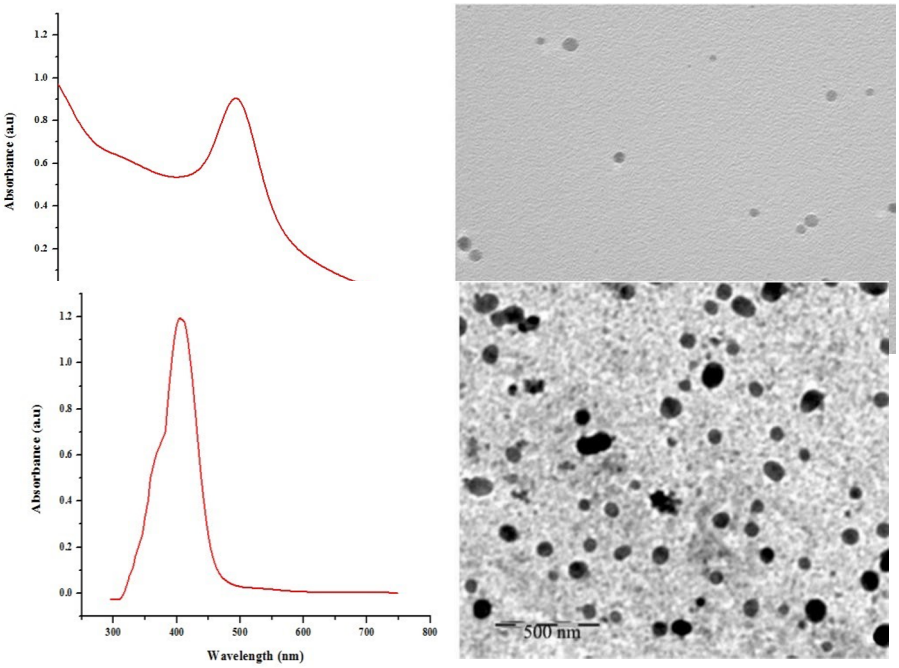

Figure 1: UV visible absorption spectrum and corresponding TEM images of **(A)** citratestabilized AuNPs and **(B)** Fe_3O_4NPs

Absorption maxima correlate with the energy difference (ΔE) or the band gap of the material under study. ΔE for any material can be calculated from the following equation

$$\Delta E = \frac{n^2 h^2}{8ml^2} \quad (1)$$

Where l corresponds to the size of the particles, Planck's constant (h), mass of the particle (m), and principal quantum number (n) .

$$E = \frac{hc}{\lambda} \quad (2)$$

$$\Delta E \propto \frac{1}{l^2} \quad (3)$$

Where c is the velocity of light and the wavelength of light absorbed (λ). Smaller is the size of the particle larger the band gap or ΔE, and hence smaller would be the wavelength of absorption.

The band gap for bulk magnetite is 0.14 eV [38], while gold, being a metal, has overlapping valence and conduction band or in other words, no band gap. Substituting the value of the absorption wavelength of gold and magnetite particles, i.e., 523 nm and 400 nm, respectively,

E_{Au}= 1239.4/523 = 2.36 eV (4)

$E_{magnetite}$ = 1239.4/400 = 3.09 eV (5)

Since the energy band gap of the synthesized materials (both gold and magnetite particles) is larger than that of the corresponding bulk materials, the synthesized particles are of much smaller dimensions, probably with structures of nanoscale dimensions. The distribution in morphology and size of these nanoparticles was further confirmed by transmission electron microscopy. TEM micrograph shows a narrow size distribution of the NPs, with Fe_3O_4 NPs having an approx. diameter ~70 nm, while AuNPs are of ~20 nm in diameter.

3.2 Optimization of parameters for GOx Activity Analysis

Structural or conformational changes due to immobilization of the enzyme lead to a reduction in its catalytic activity. The optimum temperature and pH for enzymatic activity were evaluated using different temperatures and pH levels by observing the rate of conversion of glucose. The amount of glucose left in the sample is estimated using the DNS assay. The standard curve for glucose oxidase enzyme at 37°C and pH 5.0, displayed linear response over glucose oxidase enzyme concentration ranging from 0 – 50 mU (R^2=0.994). Figure 2A shows relative activity of free enzyme GOx in phosphate buffer for pH value ranging from 5.0 to 9.0 at 37ºC. GOx shows optimum activity at pH 6.5 and more than 80% of the enzyme activity is retained for pH ranging between 5.0 and 8.0 while above pH 8.0 activity reduces drastically with only 40% activity remaining at pH 8.5.

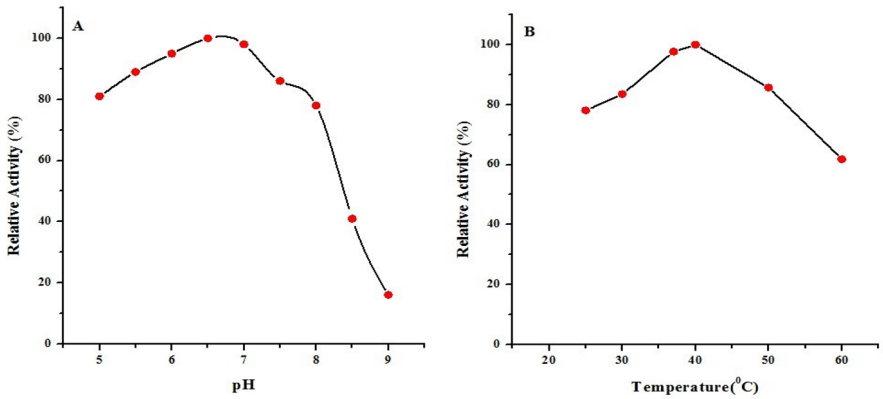

Figure 2: Relative activity of free GOx in solution with variation in (A) pH and (B) Temperature

Moreover, enzyme activity at physiological pH (i.e.7.0) is 98% of that at optimum pH (pH 6.5). Thermal stability analysis done over a temperature range of 25ºC to 60ºC (Figure 2B) showed 40ºC to be the optimum temperature.

3.3 GOx Immobilization Efficiency

The efficiency of immobilization of the enzyme was estimated for different methods and matrices, as shown in Figure 3. As seen from the bar diagram, physical adsorption methods showed poor immobilization in comparison to other methods. The enhanced percentage of covalent as well as electrostatic immobilization on nanoparticles could be attributed to the highly reactive nature of nanoparticles because of high surface energy.

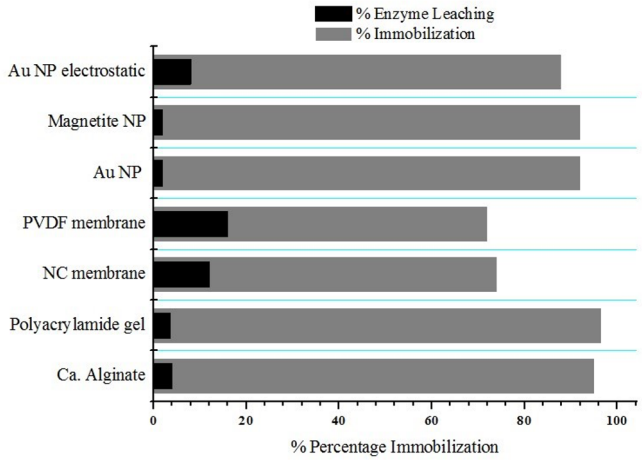

Figure 3: Comparative analysis of conventional matrices with nanomaterials for GOx immobilization in terms of immobilization and leakage percentage, respectively

Moreover, the nanoparticles not just have high surface energy, rather high surface area as well leading to high enzyme loading capacity.

Percentage loss or leakage of enzyme observed in Figure4 could be attributed to weak Van der Waals forces in case of physical adsorption in comparison to electrostatic interaction of enzyme with nanoparticles. Covalent bonding being strongest results in minimum leakage of enzyme (~2%). In case of entrapment methods enzyme leakage can be minimized by decreasing the pore size of beads and membranes or increasing the glutaraldehyde concentration in case of surface immobilization, however, this would lead to diffusional limitation and loss of enzyme activity. A balance between percentage immobilization, leakage of enzyme and effect of immobilization on activity of enzyme is the deciding factor while choosing a particular method and matrix for immobilization.

In general, if the application is of single time usage (use and throw biosensors) then electrostatic immobilization on nanoparticles could be the method of choice while for long term usage applications covalent immobilization of enzyme onto nanoparticles would be the preferred method.

3.4 Activity Analysis of Free and Immobilized Enzyme

Figure 4 shows variation of glucose concentration with time for free enzyme and GOx immobilized onto different matrices at optimum temperature (40°C). The rate of change in glucose concentration over time is generally lower for the immobilized enzyme than for the free enzyme, indicating decreased enzymatic activity in the immobilized state compared to the free solution. Rate of conversion of glucose in case of electrostatic immobilization of GOx

onto gold nanoparticles is close to that of free enzyme. The probable reasons for the observed difference in activity of GOx in each case are explained below.

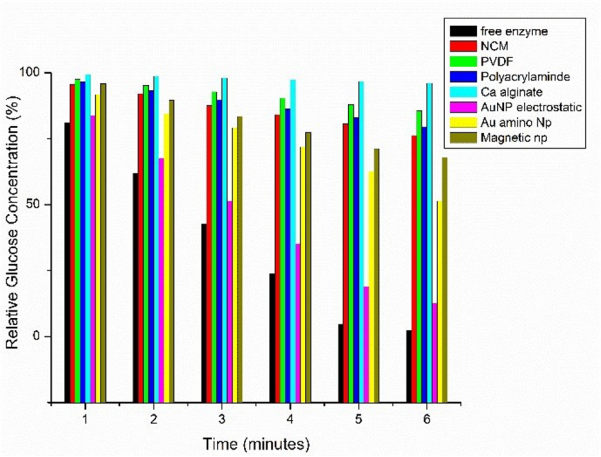

Figure 4: Variation of glucose concentration with time for free GOx in solution and GOx immobilized onto various matrices measured at 40˚C.

3.5 Adsorption of enzyme on membranes

The increased activity on NCM as compared to PVDF as observed from Figure 4 could be attributed to the nitro groups present on the NC membrane that results in activity enhancement on immobilization [39]. Moreover, NC membrane being hydrophilic in nature results in charge – charge interaction and weak secondary Van der Waals interactions with the enzyme that will not cause much damage to the structure of the enzyme as compared to the strong hydrophobic interactions in case of PVDF membrane that results in decreased enzymatic activity.

3.6 Entrapment of enzyme

It is observed that polyacrylamide gel entrapped enzyme showed larger activity than calcium alginate beads (see Figure 4). This could be attributed to the fact that polyacrylamide gel is non-ionic in nature and hence the enzyme properties would be minimally affected. However, in case of calcium alginate gel, the positively charged divalent calcium ions crosslinking the negatively charged gluconic acid residues of alginate polymer, might affect the GOx enzyme properties whose active centre is negatively charged [40]. In addition to the above, the nonionic character of polyacrylamide gel will not have much effect on diffusion of charged substrates and products, when used in an industry for production or for biosensor [41].

3.7 Electrostatic and covalent immobilization of enzyme onto nanoparticles

As shown in Figure 4, the covalent immobilization of the enzyme onto amino-functionalized AuNPs resulted in slightly lower activity compared to electrostatic immobilization on citratestabilized AuNPs of the same dimensions. This could be attributed to the stronger covalent bonds that might deform the structure of the enzyme and hence a reduced activity. However, the reduction in activity was less because of the amino functionalization of the NPs. Moreover, in case of covalent immobilization – GOx immobilized onto AuNPs showed higher activity than on Fe_3O_4NPs. This could be explained based on curvature of the nanoparticles depending on their size and adaptability (retention of conformation) of the enzyme on

immobilization. Synthesized Fe_3O_4NPs are of larger size (~70 nm) while AuNPs are of much smaller size (~20 nm) which is more suitable for immobilization of GOx enzyme (size ~5-6 nm). It was observed from the study that the interaction between the nanoparticle and protein is highly dependent on the size of the nanoparticle.

3.8 Thermal stability analysis

Thermal stability of immobilized enzyme was studied over a temperature range of 25ºC - 65ºC at pH 6.5 for each of the support matrix and method. Figure 5 (A, B) shows the relative activity (relative to maximum activity at optimum temperature) of free and immobilized GOx onto conventional and nanomaterials, respectively. As seen from

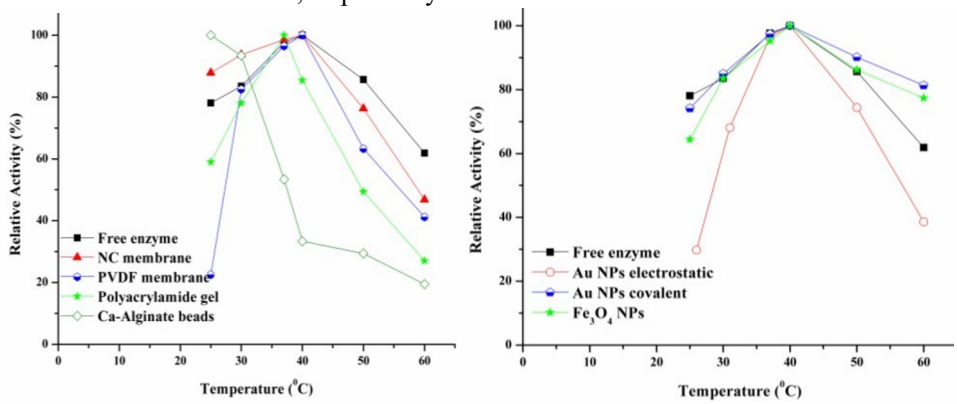

Figure 5: Thermal stability analysis of GOx immobilized onto **(A)** conventional matrices, **(B)** Thermal stability analysis of GOx immobilized on the nanomaterials.

Figure 2B, maximum activity of the immobilized GOx is at 40˚C except in case of entrapment of GOx in polyacrylamide gel and calcium alginate beads where optimum temperature was lower i.e. 37˚C and 25˚C respectively. Generally, at temperatures greater than optimum temperatures, the immobilized enzyme's activity evaluated to be less than that of the free enzyme but in the case of covalent immobilization onto nanoparticles an enhanced thermal stability of the enzyme was observed. This could be attributed to small size and appropriate curvature of the NPs [42], [43]. However, in case of electrostatic immobilization of GOx onto nanoparticles at higher temperatures activity was lower than free enzyme. This suggests that curvature and size of nanoparticles alone is not responsible for enhanced stability rather cumulative effect of covalent linkage in addition to these factors accounts for the observed trend. This is further corroborated by an exhaustive study on gold nanoparticles functionalized with different amino acids by You et al., 2005 It was shown that both hydrophobic interactions as well as the electrostatic interaction between the functionalized gold nanoparticles and proteins are responsible for stability of protein-nanoparticle complex. It was further observed that hydrophobicity binding affinity with nanoparticles and a slower rate of denaturation of proteins.

Comparison of results for immobilization efficacy, leaching of enzyme, enzyme activity and thermal stability, indicates that the nanoparticles served as better platform for immobilization as compared to traditional methods including membrane or gel entrapment. Hence, further

analysis of biosensing efficiency was done only for covalently immobilized GOx onto gold and magnetite nanoparticles.

3.9 Biosensor Sensing Efficiency Analysis

GOx-AuNPs and GOx-Fe_3O_4NPs conjugates were drop-casted on modified gold electrode for efficient detection.

3.10 Voltammetric Response

The voltammetry response of enzymatic biosensor fabricated using GOx immobilized onto Fe_3O_4NPs-gold electrode and onto AuNPs-gold electrode are shown in Figure 6 (A-C). Figure 6A represents the characteristic response of bare electrode (curve a), Fe_3O_4NPs (curve b) and AuNPs (curve c) modified electrodes in phosphate buffer (pH 7.4) at a scan rate of 100mV/s. Bare gold

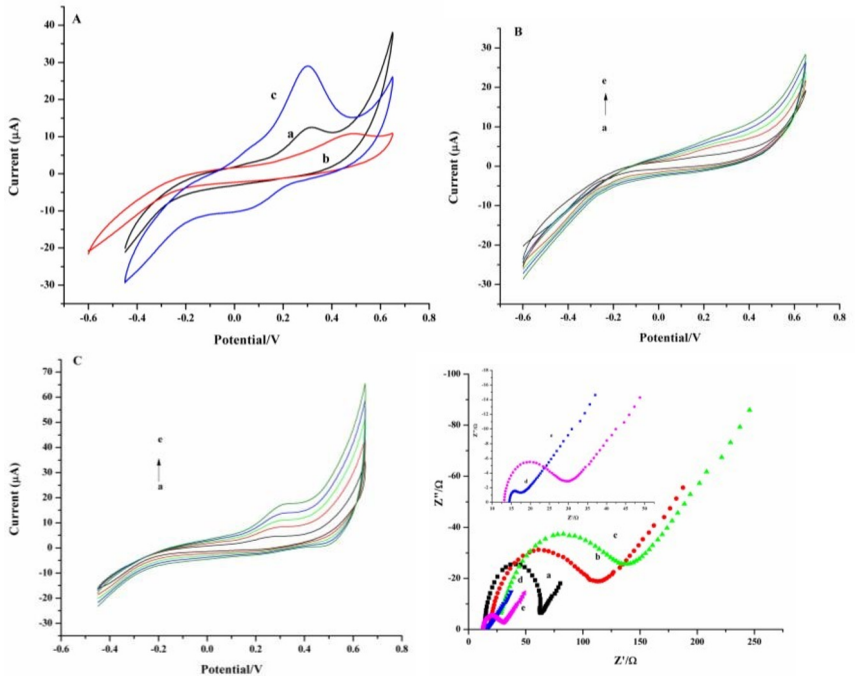

Figure 6: (A) Cyclic voltammetry (CV) of the bare electrode (curve a),Fe_3O_4 NPs with functionalized gold electrode (curve b), and the Au NPs functionalized gold electrode (curve c)in phosphate buffer solution at scan rate of 100 mV/s. **(B)** GOx-Fe_3O_4 NPs gold electrode and **(C)** GOx-Au NPs gold electrode at different scan rates and **(D)** EIS spectra of bare gold electrode (curve a), Fe_3O_4NPs functionalized gold electrode (curve b), GOx-Fe_3O_4NPs-gold electrode (curve c), AuNPs modified gold electrode (curve d), and the GOx-AuNPs-gold electrode (curve e) in solution containing 1 mM $K_3[Fe(CN)_6]$ phosphate buffer.

electrode shows a prominent reduction peak at a potential of 0.31 V however no visible oxidation peak is observed. Furthermore, modification of gold electrode surface with AuNPs is marked by a negative shift of 0.03V, at a reduction peak potential of 0.28 V with 2.6 times enhancement in peak current. A well-defined oxidation peak is observed at 0.042V.

However, Fe_3O_4 NPs modified electrodes show a much lower background current that is even less than bare gold electrode with a reduction peak at 0.49 V and peak current 3.2 times less than AuNPs modified electrode. This reduction is due to difference in material characteristics of gold and magnetite and is indicative of semiconductor type behaviour of magnetite nanoparticles. Figure 6B and 6C represent the change in behaviour after immobilization of GOx onto Fe_3O_4NPs and AuNPs modified electrode surfaces at scan rates of 20-100mV/s as shown by curve a-e respectively. Approximately two-fold reduction in current response pertaining to the insulator type behaviour of the GOx enzyme was observed. Reduction and oxidation peaks of glucose oxidase enzyme are observed at 0.24V and -0.219V respectively for Fe_3O_4NPs modified electrode. The peak-to-peak potential separation (Ep) was 0.229V at a formal potential (E°) of 0.015V. However, in case of GOx-AuNPs modified electrodes the redox peak potential of GOx is observed at 0.284V and 0.223V as seen in Figure 6C. The redox reaction of GOx (a two-electron transfer process) on the AuNP-modified electrode exhibits a Ep of **0.031 V**, indicating a reversible process. In contrast, the Fe3O4NP-modified electrode demonstrates a Ep of **0.229 V**, indicating quasi-reversible behavior. Moreover, the peak current is much higher and comparatively sharper peaks are observed in case of GOx-AuNPs modified electrodes as compared to GOx-Fe_3O_4NPs modified electrodes.

3.11 EIS Studies

The electron transfer kinetics of the redox probe is colled by the electron transfer resistance (R_{ct}) at the electrode interface. R_{ct} as calculated from Figure 7D shows that the resistance to electron transfer was lowered when a bare electrode (R_{ct} : 63Ω curve a) was modified with AuNP (R_{ct} : 18Ω, curve b) whereas the R_{ct} value increased to 30 Ω after immobilization of GOx on the surface of the modified electrode (curve c). The above results suggest that the gold nanoparticles are acting as nanoelectrodes and are helping in promoting the electron shuttling between the electrode surface and redox centre of enzyme whereas after modification of bare electrode surface with Fe_3O_4NPs the resistance to electron flow (R_{ct} : 115 Ω curve d) was even greater than bare electrode due to the semiconductor character. R_{ct} value was further increased to 140 Ω after immobilization of GOx (curve e) [44]. The increased R_{ct} after GOx immobilization in both cases (curve c and curve e) confirms the successful immobilization of GOx to the electrode acting as a barrier for the electron transfer.

3.12 Current Response

Current response for the fabricated biosensors as a function of glucose concentration at an applied voltage of 0.33V is shown in Figure 7A. The biosensor prepared by immobilization of GOx onto the Fe_3O_4NPs modified gold electrode showed 1.7 times lower current response in comparison to GOx-AuNPs-gold electrode. This could be attributed to the higher impedance of Fe_3O_4NPs as compared to AuNPs as discussed above. The calibration plot (Figure 7A) showed a linear behaviour over 1 M to 7mM glucose concentration for GOx-AuNPs-gold biosensor whereas 5 M to 5mM for GOx-Fe_3O_4NPs-gold biosensor beyond which nonlinearity set-in (Figure 7B).

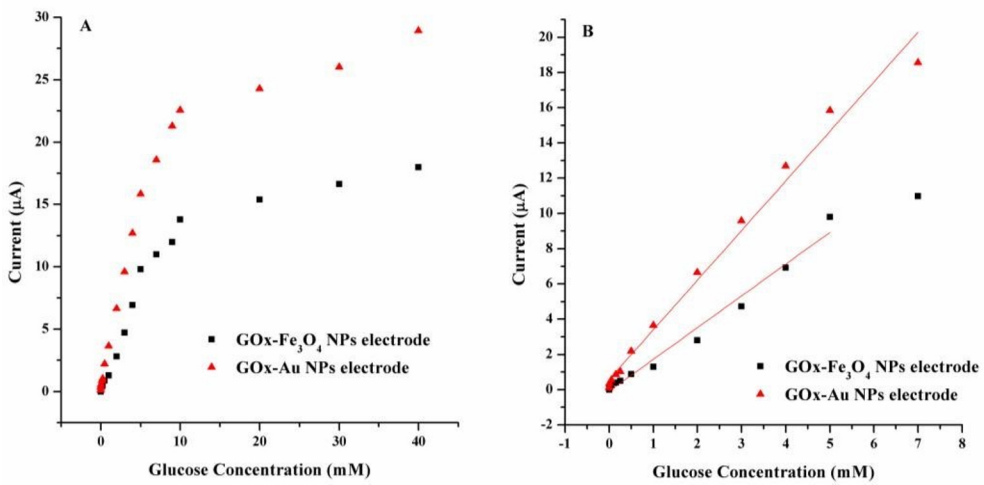

Figure 7: Amperometric response of **(A)** GOx-Fe_3O_4NPs-gold electrode and **(B)** GOxAuNPsgold electrode, to different concentrations of glucose at 0.35V in pH 7.4 phosphate buffer solution

3.13 Sensitivity and Stability

Sensitivity for the GOx-AuNPs-gold electrode is 22.42 μA mM^{-1} cm^{-2} as compared to 14.3 μA mM^{-1} cm^{-2} GOx-Fe_3O_4NPs-gold electrode [33]. The observed increase in sensitivity and current response is likely due to the biocompatibility of the amino-functionalized AuNPs, alongside their improved conductivity and lower impedance. The biocompatibility was calculated with respect to K_m that is used to measure the enzyme-substrate kinetics. K_m for Fe_3O_4NPs modified electrode was found to be 6.54 mM and 3.8 mM for AuNPs modified electrode. Figure 8 shows storage stability of biosensor measured as the current response at 25ºC for 1.0 mM glucose for a period of two months. After 60 days, the response current was found to be 73% with GOxAuNPs-gold and 56 % with GOx-Fe_3O_4NPs-gold biosensor. Long term stability and lower K_m, hence enhanced enzymatic activity, could be attributed to excellent microenvironment provided by the nanoparticles' surface, resulting in reduced leakage and denaturation of the immobilized enzyme.

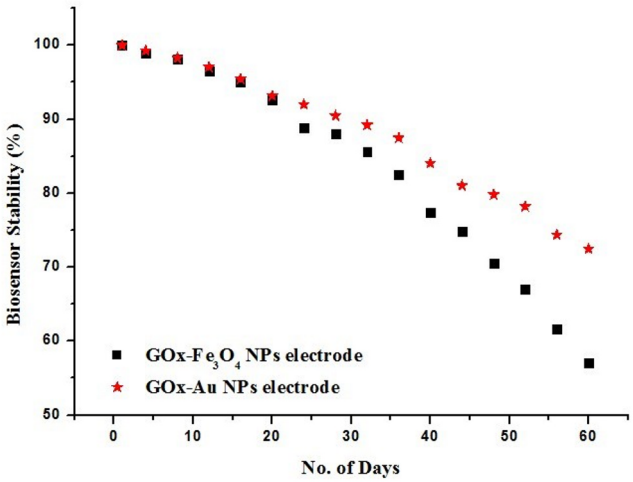

Figure 8: Storage stability of the fabricated enzymatic biosensor

Response time recorded as 4 sec and 8 sec for GOx-AuNPs-gold and GOx-Fe_3O_4NPs-gold electrodes, respectively. The low response time of the biosensors as compared to few minutes for membrane or gel-based biosensors, confirms good electro-catalytic property of the nanoparticle-based biosensor. A decrease in diffusional limitation was observed due when the size of nanoparticles were reduces resulted in rapid electron transfer between the electrode surface and the active site of immobilized enzyme.

4. Conclusion

Industrial applications exploiting catalytic capabilities of enzymes are highly dependent on method and matrix for immobilization. With ever increasing industrial needs, the research publications improvising the method of immobilization or designing newer matrices are also increasing dramatically. However, no comparative study presenting the efficiency of these immobilization techniques and matrices have been reported till date. Our comparative analysis of various immobilization methods revealed that while electrostatic immobilization minimizes enzyme denaturation, covalent attachment to the nanoparticle surface provides the storage and operational stability required for industrial biosensors. Moreover, covalent immobilization onto suitably functionalized nanoparticles, depending on properties of the chosen enzyme in general and specially that of active site residues, results in optimum immobilization and maximization of catalytic activity. In other words, synergistic effect of appropriate functionalization and size of nanoparticles promotes thermal stability as well as operational stability and high sensitivity of the biosensor. Nonetheless, the electrostatic or covalent method of immobilization remains a commercial decision.

References

[1] L. C. Clark Jr. and C. Lyons, "Electrode systems for continuous monitoring in cardiovascular surgery," *Ann. N. Y. Acad. Sci.*, vol. 102, no. 1, pp. 29–45, 1962, doi: https://doi.org/10.1111/j.1749-6632.1962.tb13623.x.

[2] A. Shahbaz, N. Hussain, A. Intisar, M. Bilal, and H. M. N. Iqbal, "Immobilized Enzymes-Based Biosensing Cues for Strengthening Biocatalysis and Biorecognition," *Catal. Letters*, vol. 152, no. 9, pp. 2637–2649, 2022, doi: 10.1007/s10562-021-038664.

[3] M. S. Robescu and T. Bavaro, "A Comprehensive Guide to Enzyme Immobilization: All You Need to Know," Feb. 01, 2025, *Multidisciplinary Digital Publishing Institute (MDPI)*. doi: 10.3390/molecules30040939.

[4] K. Sirkar, A. Revzin, and M. V Pishko, "Glucose and Lactate Biosensors Based on Redox Polymer/Oxidoreductase Nanocomposite Thin Films," *Anal. Chem.*, vol. 72, no. 13, pp. 2930–2936, Jul. 2000, doi: 10.1021/ac991041k.

[5] W.-L. Zhu, Y. Zhou, and J.-R. Zhang, "Direct electrochemistry and electrocatalysis of myoglobin based on silica-coated gold nanorods/room temperature ionic liquid/silica sol–gel composite film," *Talanta*, vol. 80, no. 1, pp. 224–230, 2009, doi: https://doi.org/10.1016/j.talanta.2009.06.056.

[6] K. Berketa *et al.*, "Amperometric Biosensor Based on a Semipermeable PolyMetaPhenylenediamine Membrane and Immobilized Lactate Oxidase for Highly Accurate l-Lactate Determination in Blood Serum," *Electroanalysis*, vol. 37, no. 1, p. e12011, Jan. 2025, doi: https://doi.org/10.1002/elan.12011.

[7] A. E. G. Cass *et al.*, "Ferrocene-mediated enzyme electrode for amperometric determination of glucose," *Anal. Chem.*, vol. 56, no. 4, pp. 667–671, Apr. 1984, doi: 10.1021/ac00268a018.

[8] J. Zdarta, A. S. Meyer, T. Jesionowski, and M. Pinelo, "A General Overview of Support Materials for Enzyme Immobilization: Characteristics, Properties, Practical Utility," *Catalysts*, vol. 8, no. 2, 2018, doi: 10.3390/catal8020092.

[9] M. Wang *et al.*, "Advancements in magnetic nanoparticle-based biosensors for pointofcare testing," *Front. Bioeng. Biotechnol.*, vol. Volume 12-2024, 2024, doi: 10.3389/fbioe.2024.1393789.

[10] Y. Ge *et al.*, "Glucose oxidase complexed gold-graphene nanocomposite on a dielectric surface for glucose detection: A strategy for gestational diabetes mellitus," *Int. J. Nanomedicine*, vol. 14, pp. 7851–7860, 2019, doi: 10.2147/IJN.S222238.

[11] V. Gigli, C. Tortolini, E. Capecchi, A. Angeloni, A. Lenzi, and R. Antiochia, "Novel Amperometric Biosensor Based on Tyrosinase/Chitosan Nanoparticles for Sensitive and Interference-Free Detection of Total Catecholamine," *Biosensors (Basel).*, vol. 12, no. 7, p. 519, Jul. 2022, doi: 10.3390/bios12070519.

[12] N. Yildirim-Tirgil, S. Akkoyun, H. U. Atan, and B. Bozkurt, "Development of a Polypyrrole–Chitosan Electrospun Nanofiber-Based Enzymatic Biosensor for Sensitive and Rapid Detection of Acetylcholine," *ACS Appl. Polym. Mater.*, vol. 7, no. 2, pp. 611–621, Jan. 2025, doi: 10.1021/acsapm.4c02614.

[13] X. Jin, G. Li, T. Xu, L. Su, D. Yan, and X. Zhang, "Fully integrated flexible biosensor for wearable continuous glucose monitoring," *Biosens. Bioelectron.*, vol. 196, p. 113760, Jan. 2022, doi: 10.1016/j.bios.2021.113760.

[14] P. Yari et al., "Magnetic Particle Spectroscopy for Point-of-Care: A Review on Recent Advances," *Sensors*, vol. 23, no. 9, p. 4411, 2023, doi: 10.3390/s23094411.G. Fortier, E. Brassard, and D. Bélanger, "Optimization of a polypyrrole glucose oxidase biosensor," *Biosens. Bioelectron.*, vol. 5, no. 6, pp. 473–490, 1990, doi: https://doi.org/10.1016/0956-5663(90)80036-D.

[15] W. Kerner *et al.*, "A potentially implantable enzyme electrode for amperometric measurement of glucose.," *Horm. Metab. Res. Suppl.*, vol. 20, pp. 8–13, 1988.

[16] D. Quan, R. K. Nagarale, and W. Shin, "A Nitrite Biosensor Based on Coimmobilization of Nitrite Reductase and Viologen-Modified Polysiloxane on Glassy Carbon Electrode," *Electroanalysis*, vol. 22, no. 20, pp. 2389–2398, Oct. 2010, doi: 10.1002/elan.200900634.

[17] S. F. D'Souza, J. Kumar, S. K. Jha, and B. S. Kubal, "Immobilization of the urease on eggshell membrane and its application in biosensor," *Materials Science and Engineering: C*, vol. 33, no. 2, pp. 850–854, Mar. 2013, doi: 10.1016/j.msec.2012.11.010.

[18] M. Şenel, "Simple method for preparing glucose biosensor based on in-situ polypyrrole cross-linked chitosan/glucose oxidase/gold bionanocomposite film," *Materials Science and Engineering: C*, vol. 48, pp. 287–293, Mar. 2015, doi: 10.1016/j.msec.2014.12.020.

[19] P. Barathi, B. Thirumalraj, S.-M. Chen, and S. Angaiah, "A simple and flexible enzymatic glucose biosensor using chitosan entrapped mesoporous carbon nanocomposite," *Microchemical Journal*, vol. 147, pp. 848–856, 2019, doi: https://doi.org/10.1016/j.microc.2019.03.083.

[20] C. Yan, K. Jin, X. Luo, J. Piao, and F. Wang, "Electrochemical Biosensor Based on Chitosan- and Thioctic-Acid-Modified Nanoporous Gold Co-Immobilization Enzyme for Glycerol Determination," *Chemosensors*, vol. 10, no. 7, p. 258, Jul. 2022, doi: 10.3390/chemosensors10070258.

[21] M. Artigues, J. Abellà, and S. Colominas, "Analytical Parameters of an Amperometric Glucose Biosensor for Fast Analysis in Food Samples," *Sensors*, vol. 17, no. 11, 2017, doi: 10.3390/s17112620.

[22] Y. Bai, H. Yang, W. Yang, Y. Li, and C. Sun, "Gold nanoparticles-mesoporous silica composite used as an enzyme immobilization matrix for amperometric glucose

biosensor construction," *Sens. Actuators B Chem.*, vol. 124, no. 1, pp. 179–186, Jun. 2007, doi: 10.1016/j.snb.2006.12.020.

[23] V. Narwal and C. S. Pundir, "Development of glycerol biosensor based on coimmobilization of enzyme nanoparticles onto graphene oxide nanoparticles decorated pencil graphite electrode," *Int. J. Biol. Macromol.*, vol. 127, pp. 57–65, 2019, doi: https://doi.org/10.1016/j.ijbiomac.2018.12.253.

[24] J. Zhu *et al.*, "Microarray H2O2 electrodes as base elements of high-response glucose sensors," *Sens. Actuators B Chem.*, vol. 20, no. 1, pp. 17–22, 1994, doi: https://doi.org/10.1016/0925-4005(93)01166-2.

[25] X. Ren, D. Chen, X. Meng, F. Tang, A. Du, and L. Zhang, "Amperometric glucose biosensor based on a gold nanorods/cellulose acetate composite film as immobilization matrix," *Colloids Surf. B Biointerfaces*, vol. 72, no. 2, pp. 188–192, 2009, doi: https://doi.org/10.1016/j.colsurfb.2009.04.003.

[26] M. M. Barsan *et al.*, "Direct Immobilization of Biomolecules through Magnetic Forces on Ni Electrodes via Ni Nanoparticles: Applications in Electrochemical Biosensors," *ACS Appl. Mater. Interfaces*, vol. 11, no. 22, pp. 19867–19877, Jun. 2019, doi: 10.1021/acsami.9b04990.

[27] Y.-Y. Li *et al.*, "Glucose Biosensor Based on Glucose Oxidase Immobilized on BSA Cross-Linked Nanocomposite Modified Glassy Carbon Electrode," *Sensors*, vol. 23, no. 6, p. 3209, Mar. 2023, doi: 10.3390/s23063209.

[28] K. Sakdaphetsiri, S. Teanphonkrang, and A. Schulte, "Cheap and Sustainable Biosensor Fabrication by Enzyme Immobilization in Commercial Polyacrylic Acid/Carbon Nanotube Films," *ACS Omega*, vol. 7, no. 23, pp. 19347–19354, Jun. 2022, doi: 10.1021/acsomega.2c00925.

[29] X. Tong, L. Jiang, Q. Ao, X. Lv, Y. Song, and J. Tang, "Highly stable glucose oxidase polynanogel@MXene/chitosan electrochemical biosensor based on a multi-stable interface structure for glucose detection," *Biosens. Bioelectron.*, vol. 248, p. 115942, Mar. 2024, doi: 10.1016/j.bios.2023.115942.

[30] Y. Zhu and Q. Wu, "Synthesis of Magnetite Nanoparticles by Precipitation with Forced Mixing," *Journal of Nanoparticle Research*, vol. 1, no. 3, pp. 393–396, 1999, doi: 10.1023/A:1010091625981.

[31] J. Turkevich, P. C. Stevenson, and J. Hillier, "A study of the nucleation and growth processes in the synthesis of colloidal gold," *Discuss. Faraday Soc.*, vol. 11, no. 0, pp. 55–75, 1951, doi: 10.1039/DF9511100055.

[32] S. Sharma, N. Gupta, and S. Srivastava, "Modulating electron transfer properties of gold nanoparticles for efficient biosensing," *Biosens. Bioelectron.*, vol. 37, no. 1, pp. 30–37, 2012, doi: https://doi.org/10.1016/j.bios.2012.04.027.

[33] J. M. González-Sáiz and C. Pizarro, "Polyacrylamide gels as support for enzyme immobilization by entrapment. Effect of polyelectrolyte carrier, pH and temperature

on enzyme action and kinetics parameters," *Eur. Polym. J.*, vol. 37, no. 3, pp. 435– 444, Mar. 2001, doi: 10.1016/S0014-3057(00)00151-8.

[34] H.-Ui. Bergmeyer, *Methods of enzymatic analysis*. Elsevier, 2012.

[35] K.-J. Chen, C.-F. Lee, J. Rick, S.-H. Wang, C.-C. Liu, and B.-J. Hwang, "Fabrication and application of amperometric glucose biosensor based on a novel PtPd bimetallic nanoparticle decorated multi-walled carbon nanotube catalyst," *Biosens. Bioelectron.*, vol. 33, no. 1, pp. 75–81, 2012.

[36] S. Sharma, A. Shrivastav, N. Gupta, and S. Srivastava, "Amperometric Biosensor: Increased Sensitivity Using Enzyme Nanoparticles."

[37] E. Krishnakanth and P. M. Kumar, "Enhanced Electrochemical Performance of TiO_2 Thin Films Modified with CQD@Fe_3O_4 Nanocomposites," *Journal of Mines, Metals and Fuels*, pp. 93–107, Jan. 2026, doi: 10.18311/jmmf/2026/52871.

[38] J. C. Tiller, R. Rieseler, P. Berlin, and D. Klemm, "Stabilization of activity of oxidoreductases by their immobilization onto special functionalized glass and novel aminocellulose film using different coupling reagents," *Biomacromolecules*, vol. 3, no. 5, pp. 1021–1029, 2002.

[39] A. Blandino, M. Macıas, and D. Cantero, "Immobilization of glucose oxidase within calcium alginate gel capsules," *Process Biochemistry*, vol. 36, no. 7, pp. 601–606, 2001.

[40] J. R. Retama, B. Lopez-Ruiz, and E. Lopez-Cabarcos, "Microstructural modifications induced by the entrapped glucose oxidase in cross-linked polyacrylamide microgels used as glucose sensors," *Biomaterials*, vol. 24, no. 17, pp. 2965–2973, 2003.

[41] C.-C. You, M. De, G. Han, and V. M. Rotello, "Tunable inhibition and denaturation of α-chymotrypsin with amino acid-functionalized gold nanoparticles," *J. Am. Chem. Soc.*, vol. 127, no. 37, pp. 12873–12881, 2005.

[42] M. Lundqvist, I. Sethson, and B.-H. Jonsson, "Protein adsorption onto silica nanoparticles: conformational changes depend on the particles' curvature and the protein stability," *Langmuir*, vol. 20, no. 24, pp. 10639–10647, 2004.

[43] S. Sharma and S. Srivastava, "Gold microwires based amperometric biosensor exploiting microbial architecture," *Biosens. Bioelectron.*, vol. 50, pp. 174–179, 2013.